Prediction of Glass Transition Temperature (T_g) of Some Compounds in Organic Electroluminescent Devices with Their Molecular Properties

Yeong Suk Kim,[†] Jae Hyun Kim,*[,⊥] Jung Sup Kim,[#] and Kyoung Tai No[#,‡,§]

Department of Chemistry and Department of Chemical Education, Kongju National University, Kongju 314-700, Korea, and Computer Aided Molecular Design Research Center and Department of Bioinformatics and Department of Chemistry, Soong Sil University, Seoul 156-743, Korea

Received June 12, 2001

We have studied the quantitative structure−property relationship between descriptors representing the molecular structure and glass transition temperature (T_g) for 103 molecules including organic electroluminescent (EL) devices materials. Eighty-six descriptors were introduced and among them seven descriptors (one topological descriptor, one thermodynamic descriptor, one spatial descriptor, one structural descriptor, and three electrostatic descriptors) were selected by Genetic Algorithm (GA). The 81 molecules chosen randomly among 103 compounds were used as a training set, and the remaining 22 molecules were used as a prediction set. The quantitative relationship between these seven descriptors and T_g was tested by multiple linear regression (MLR) and artificial neural network (ANN). ANN analysis showed no significant advantage over MLR for this study. As the results of the MLR, the square of the correlation coefficient (R^2) for the T_g of the 81 training set was 0.989, and the average error was 8.8 K. In prediction for T_g using the 22 prediction compounds set with MLR, R^2 was 0.976, and the average error was 13.9 K.

INTRODUCTION

Glass transition generally occurs over a relatively narrow temperature region and is similar to the solidification of a liquid to a glassy state; it is not a phase transition. Many liquids, upon sufficient supercooling below their freezing points, exhibit a glass transition temperature (T_g) at which certain properties of the liquid such as the coefficient of thermal expansion and the heat capacity change from their liquid-state values to values similar to those of a crystalline solid. Structural relaxation of a liquid in response to changes in the external thermodynamic variables such as temperature, pressure, shear stress, or electric field is the origin of glass transition. T_g can be determined readily by observing the temperature region at which a significant change takes place in the external thermodynamic variables. The definition of glass transition and the glass transition temperature are described well in the American Society for Testing and Materials (ASTM) report.[1]

The T_g is one of the most crucial properties of polymers. As most of the polymers are so huge, the numbers of sectors having the required conditions for crystallization is not satisfactory, though the linear polymers are simple in their structure. That is, if an amorphous sector exists, crystallization does not occur. However, as the temperature decreases, the total energy of the polymer chain decreases, and the twisting motion by the rotational bond axes freezes. Then, the polymers become rigid like glass and fragile. To illuminate and describe the relationship between the physical properties of the polymers and T_g, several operations have been performed.[2−13]

Several kinds of quantitative structure−property relationship (QSPR) models were proposed depending on the expression of the descriptors in QSPR equations. As a popular approach, the T_g of polymers is expressed with the MLR equation of the descriptors, which are based on the concept of group additivity property (GAP). That is, according to the GAP concept, a physicochemical property of the chemical system is simply the scalar sum of the respective individual physicochemical properties of the component chemical groups.[3] Since the groups in a polymer influence each other through both space and chemical bonds, the group additivity methods are limited in expressing this effect. And the group additivity methods are not applicable to predictions for the polymers containing previously noninvestigated groups.

To overcome these limitations, Hopfinger et al.[4,5] introduced computer modeling in addition to the group additivity approach. According to this approach, the conformational entropy associated with torsional rotations is a predominant factor in determining T_g.

Bicerano[7] introduced the atomic or bond connectivity indices as the descriptors of the QSPR expression. In the EVM (energy, volume, and mass) model, atomistic simulation is combined with the classical QSPR method. It was the available database of molecular mechanics and a molecular dynamics simulation, through which descriptors for the QSPR equation were derived.

For the practical use of the EL materials to organic emitting diodes (OLED), as a physical property, the compound must have high T_g. High T_g materials satisfy the

* Corresponding author phone: 82-41-850-8281; fax: 82-41-850-8347; e-mail: kjaehyun@kongju.ac.kr.
[†] Department of Chemistry, Kongju National University.
[⊥] Department of Chemical Education, Kongju National University.
[#] Computer Aided Molecular Design Research Center, Soong Sil University.
[‡] Department of Bioinformatics and Department of Chemistry, Soong Sil University.
[§] Member of Hyperstructural Organic Material Research Center, Korea.

10.1021/ci0103018 CCC: $22.00
Published on Web 01/28/2002

Table 1. Comparison between Experimental and Predicted T_g Values of 81 Organic Molecules Used as the Training Set[d]

no.	compound	exp. T_g(K)	pre. T_g(K)	no.	compound	exp. T_g(K)	pre. T_g(K)
1	2-methylpentane[17]	80	77	42	triethylamine[22]	103	105
2	3-methylhexane[17]	88	81	43	acetoamine[23]	91	109
3	2,3-dimethylbutane[18]	76	78	44	2-bromobutane[17]	97	99
4	ethylcyclohexane[19]	98	104	45	1,2-difluorotetrachloroethane[26]	90	102
5	isopropylcyclohexane[19]	108	109	46	isobutylbromide[19]	95	98
6	*n*-hexylcyclohexane[19]	133	126	47	isoamylbromide[19]	105	98
7	methylcyclohexane[19]	85	100	48	carbontetrachloride[27]	130	124
8	*sec*-butylcyclohexane[19]	123	112	49	chloroform[27]	105	123
9	*n*-butylcyclohexane[19]	119	114	50	benzaldehyde[22]	149	147
10	*n*-pentylcyclohexane[19]	125	120	51	acetophenone[22]	161	156
11	1-heptene[19]	91	95	52	acetone[13]	100	104
12	2-methyl-2-butene[17]	73	88	53	methylethyl ketone[22]	111	103
13	cis-oct-2-ene[19]	101	95	54	methylisobutyl ketone[22]	120	113
14	1-hexene[19]	83	90	55	isopropyl ether[22]	101	104
15	cis-hept-2-ene[19]	93	91	56	dimethylphthalate[19]	193	190
16	trans-hex-2-ene[19]	85	89	57	di-*n*-butylphthalate[19]	176	190
17	toluene[20]	115	118	58	di-(2-ethylhexyl)phthalate[19]	184	197
18	*sec*-butylbenzene[19]	127	126	59	ethyl acetate[22]	118	122
19	ethylbenzene[19]	111	121	60	propylenecarbonate[28]	160	143
20	isopropylbenzene[20]	125	125	61	dimethyl sulfoxide[22]	150	125
21	*tert*-butylbenzene[19]	142	128	62	pyridine[22]	127	130
22	*n*-butylbenzene[19]	125	127	63	dimethylformamide[17]	129	124
23	*n*-propylbenzene[19]	122	126	64	1,1′- di(paramethoxy,metamethylphenyl)cyclohexane[29]	261	240
24	*n*-pentylbenzene[19]	128	135	65	1,1′- di(paramethoxylphenyl)cyclohexane[29]	240	238
25	*n*-hexylbenzene[19]	137	140	66	TPD[14,a,b]	338	339
26	*m*-xylene[20]	126	124	67	ETCz2[14,a]	343	328
27	o-terphenyl[21]	243	212	68	PHCZ2[14,a]	363	371
28	ethanol[22]	97	109	69	p-TTA[31,a]	405	380
29	methanol[23]	103	102	70	AODF1[32,a]	353	357
30	1-butanol[22]	112	116	71	AODF5[32,a]	455	440
31	1-hexanol[22]	130	126	72	EM1[33,a]	407	383
32	1-pentanol[22]	121	121	73	EM2[33,a]	395	415
33	glycerol[19]	186	194	74	EM4[33,a]	372	376
34	ethyleneglycol[17]	154	151	75	TCTA[34,b]	424	439
35	propyleneglycol[24]	167	152	76	m-MTDAPB[34,b]	378	372
36	cyclohexanol[18]	150	136	77	1-TNATA[34,b]	386	394
37	salol[25]	213	235	78	bis[2′-(2,4,6-tripheny-1,3,5-triazinyl)] ethers 3a[36,c]	379	405
38	benzyl alcohol[17]	171	161	79	bis[2′-(2,4,6-tripheny-1,3,5-triazinyl)] ethers 3c[36,c]	412	417
39	cyclooctanol[18]	168	143	80	bis[2′-(2,4,6-tripheny-1,3,5-triazinyl)] ethers 3d[36,c]	406	408
40	cyanoadamantane[18]	170	188	81	bis[2′-(2,4,6-tripheny-1,3,5-triazinyl)] ethers 3e[36,c]	417	402
41	cyanocyclohexane[18]	135	131				

[a] Emitting molecule. [b] Hole transport molecule. [c] Hole blocking/electron transport molecule. [d] The predicted T_gs were calculated with eq 2. From compound nos. 66 to 81, the compound names were taken from the references.

requirements for the practical applications of OLED: (1) elaboration of thermally stable thin organic films and (2) fabrication of highly stable contacts between organic films and electrodes.[14,15] Degradation of the OLED is primarily caused by the morphological changes of the amorphous organic layers, especially, at the hole transporting layer.

The purpose of this work is (1) to discover the physical properties which significantly influence the T_g of organic molecules, (2) to obtain the relationship between the physical properties of organic molecules and their T_g, and (3) to apply the obtained relationship to predict the T_g of LED materials.

COMPUTATION

A. Database Construction. The 103 organic compounds summarized in Tables 1 and 2 were introduced for the QSPR study, the relationship between molecular structure and T_g. The compounds 1−65 and 82−95 are the fragments or possible fragments of EL compounds. Among the 103 molecules, 24 molecules are LED materials. Among 24 LED materials, 16 compounds were included in training set, and the other compounds were included in test set.

The T_gs of the data set compounds have values between 73 and 455 K. Particularly, the T_gs of the LED materials lie between 338 and 455 K. The structures of LED materials are depicted in Figure 1.

Since many of the descriptors that will be introduced for the QSPR studies are three-dimensional properties of the molecules, the physically realistic three-dimensional structures of the molecules are necessary for the reliability of the QSPR results. The three-dimensional structures of the compounds were obtained by an energy minimization procedure, and the energies of the molecules were calculated by Merck Molecular Force Field (MMFF).[16]

The experimental T_g values were taken from several works.[14,17−36]

B. Calculation of Molecular Descriptors. In all, 86 descriptors were calculated for each compound. These 86 descriptors can be classified into five groups: topological, spatial, electrostatic, thermodynamic, and structural descriptors.

The topological descriptors were represented by the Wiener index,[37] Randic indices,[38] and Kier-Hall indices,[39]

Table 2. Comparison between Experimental and Predicted T_g Values of 22 Organic Molecules Used as the Prediction Set[d]

no.	compound	exp. T_g(K)	pre. T_g(K)	no.	compound	exp. T_g(K)	pre. T_g(K)
82	2-methylbutane[17]	76	72	93	diethyl ether[22]	92	103
83	acetonitrile[17]	93	106	94	a-penyl-*o*-cresol[25]	210	201
84	4-methylcyclohexene[17]	94	108	95	1,3,5-tri-a-naphthylbenzene[25]	334	330
85	benzene[17]	131	111	96	TPTE[14,b]	403	405
86	acetaldehyde[17]	82	105	97	AODF2[32,a]	353	336
87	trifluroethanol[17]	144	157	98	EM3[33,a]	391	399
88	di-isobutylphthalate[19]	188	192	99	EM5[33,a]	440	364
89	isobutyl chloride[19]	88	102	100	m-MTDATA[34,b]	348	367
90	*trans*-1,2-dimethylcyclohexane[20]	97	106	101	2-TNATA[34,b]	383	384
91	dimethylacetamide[22]	146	127	102	NPB[35,b]	368	376
92	1-propanol[22]	121	112	103	bis[2′-(2,4,6-triphenyl-1,3,5-triazinyl)] ethers 3b[36,c]	388	378

[a] Emitting molecule. [b] Hole transport molecule. [c] Hole blocking/electron transport molecule. [d] The predicted T_gs were calculated with eq 2. From compound nos. 96 to 103, the compound names were taken from the references.

which describe the branching of molecules, providing virtually identical information.

The radius of gyration, density, and volume were introduced as the spatial descriptors.

A subclass of electrostatic descriptors, called charged partial surface area (CPSA) descriptors, were introduced by Jurs et al.[40,41] A set of 30 CPSA descriptors is calculated as a combination of the contributions of atomic partial charges to the total molecular solvent-accessible surface area. The CPSA descriptors encode information regarding intermolecular interactions such as hydrogen bonding or polar interactions.

As thermodynamic descriptors, AlogP (logarithm value of the partition coefficient of the compound between 1-octanol and water), desolvation free energy for water, desolvation free energy for octanol, heat of formation, and molar refractivity were calculated on the basis of the total partition function of the molecule and its electronic, translational, rotational, and vibrational components.

The structural descriptors were composed of molecular weight, number of rotational bonds, and number of hydrogen bond acceptors and donors.

C. Determination of Optimum Descriptor Set. Though several optimum descriptor sets to predict the T_g of polymers were proposed by several workers,[2−13] the descriptors which contributed significantly to the T_g were selected from the descriptors pool, because the motions influential to the T_g may be quite different between polymers and organic molecules. The genetic algorithm (GA) that is a class of methods based on biological evolution was used for the selection of the optimum descriptors set. The first step is to create a population of linear regression models. These regression models mate with each other, mutate, crossover, reproduce, and then evolve through successive generations toward an optimum solution. The optimum descriptors for describing the T_g of organic molecules were obtained with the GA.

The GA simulation conditions are 10 000 generations and 100 populations. And the equation of each string is described as a linear combination of 4−12 descriptors. The GA procedure was repeated nn-times to confirm that the selected descriptors are the most optimal descriptor set for describing the T_g of the EL compounds.

The 'reliability' of a regression equation is often represented with the square of the correlation coefficient (R^2). During the evolution of the GA, the fitness was calculated as follows

$$R^2 = 1 - \frac{\sum_{i=1}^{n} (T_{g,i}^{obs} - T_{g,i}^{pre})^2}{\sum_{i=1}^{n} (T_{g,i}^{obs} - \bar{T}_g)^2} \quad (1)$$

where i represents ith molecule, and $T_{g,i}^{obs}$, $T_{g,i}^{pre}$, and $\bar{T}g$ represent the observed, predicted ,and average values of the T_g, respectively.

RESULTS AND DISCUSSION

Among 103 compounds in the data set, 81 compounds were randomly selected for the training set (Table 1), and the remaining 22 compounds were used for the prediction set (Table 2).

To reduce the number of descriptors to an acceptable subset size that contained the most important information, the genetic algorithm[42] was employed. Numerous MLR models were created using some descriptors that were selected by the genetic algorithm. The MLR models can have 4−12 descriptors in the equations. The quality was measured by the square of the cross-validation correlation coefficient (R_{cv}^2) and the square of the correlation coefficient (R^2).

In general, it is believed that the artificial neural network (ANN) is superior to the linear regression method in its capacity to handle nonlinear correlation effects. Therefore the ANN was trained with the same descriptors as the MLR to reproduce the experimental T_gs. However, according to the results, ANN analysis has no significant advantage over MLR for T_g prediction. It seems that the descriptors selected through the GA procedure are not much correlated each other.

According to the R^2 value of each model, seven descriptors are enough to describe the T_g. As an optimum descriptors set, seven descriptors that appear with high probability during the GA procedure were selected (Table 3). To test the dependency of the T_g on each physical property, descriptor, R^2, R_{cv}^2, and the average error (AE) were calculated with one descriptor linear regression (LR) with the 81 training compounds set.

The SC-1 descriptor gave the best overall fit with the R^2 value of 0.909 for the whole 81 training set. The number of

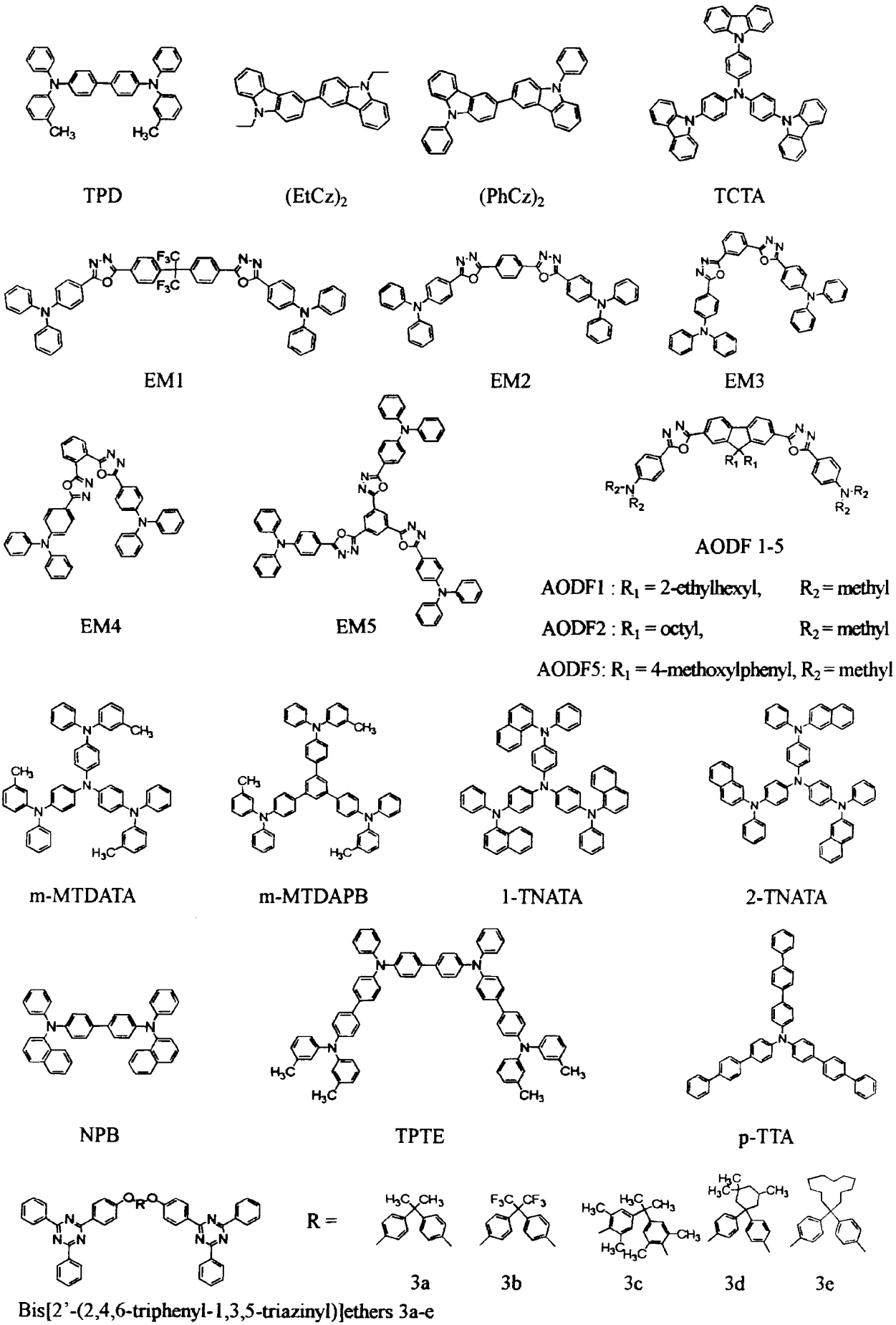

Figure 1. Organic EL devices materials included in the training and prediction set.

Table 3. Descriptors Involved in the Best Seven-Parameter Model Derived for T_g[a]

descriptor name	descriptor type	definition
SC-1	topological	no. of bonds
AlogP	thermodyn	octanol/water partition coeff
RadofGyration	spatial	radius of gyration
HBC	structural	min. no. between the no. of H acceptor and the no. of H donor
WNSA-1	electrostatic	surface weighted negative charged partial surface area
FPSA-2		fractional positive charged partial surface area
TPSA		total polar surface area

[a] SC-1: first-order Kier and Hall subgraph count index, which is the number of edges (bonds) that connect the vertices (atoms) of the molecular graph. AlogP: calculated using the method described by Ghose and Crippen. RadofGyration:

$$\mathrm{RoG} = \sqrt{\left(\sum \frac{(x_i^2 + y_i^2 + z_i^2)}{N}\right)}$$

where N is the number of atoms and x, y, and z are the atomic coordinates relative to the center of mass. HBC: $\min(H_a, H_d)$ where H_a is the number of H acceptors, and H_d is the number of H donors. WNSA-1: surface weighted negative charged partial surface area obtained partial negative (surface area multiplying total molecular solvent area and dividing by 1000) WNSA $-$ 1 $= (\sum(-\mathrm{SA}_i)(\mathrm{TMSA}))/1000$ where $-\mathrm{SA}_i$ is the surface area contributions of the ith negative atom in the molecule, and TMSA is the total molecular surface area. FPSA-2: fractional positive charged partial surface area obtained total charge weighted positive surface area divided by the total molecular solvent accessible surface area FPSA $-$ 2 $= (\sum(+\mathrm{SA}_i))Q^+_T)/(\mathrm{TMSA})$ where $+\mathrm{SA}_i$ is the surface area contributions of the ith positive atom in the molecule, TMSA is the total molecular surface area, and Q^+_T is the sum total positive charges for the molecule. TPSA: sum of solvent-accessible surface areas of atoms with an absolute value of partial charges greater than or equal to 0.2.

Table 4. Summary of One Descriptor Models for 81 Training Set

descriptor	T_g prediction equation	R^2	R_{cv}^2	AE (K)
SC-1	$T_g = (4.233 \times \mathrm{SC\text{-}1}) + 96.984$	0.909	0.904	26.6
RoG	$T_g = (42.824 \times \mathrm{RoG}) + 24.825$	0.857	0.852	35.0
WNSA-1	$T_g = (0.493 \times \mathrm{WNSA\text{-}1}) + 123.897$	0.816	0.805	34.6
AlogP	$T_g = (18.730 \times \mathrm{AlogP}) + 92.676$	0.789	0.783	41.1
FPSA-2	$T_g = (50.050 \times \mathrm{FPSA\text{-}2}) + 68.147$	0.657	0.654	50.2
TPSA	$T_g = (0.667 \times \mathrm{TPSA}) + 138.058$	0.133	0.062	78.2
HBC	$T_g = (-21.787 \times \mathrm{HBC}) + 96.984$	0.012	−0.032	88.4

first-order subgraphs (SC-1) in a molecular graph is the number of edges that connect the vertices of the molecular graph. In other words, it is the number of the bonds in a molecule and is roughly linear depending on the size of the molecule.

When the T_g was calculated with only the SC-1 descriptor, the AE of T_g was 26.6 K, the calculated T_g was above the estimate for the experimental T_g for hydrocarbons, and the calculated T_g was below the estimate for the experimental T_g for alcohols. It is evident that the T_g increases substantially if the molecule can form a hydrogen bond which its neighbor. The T_gs of methanol (T_g = 103 K) and cyclohexanol (T_g = 150 K) are higher than the T_g of 2-methylbutane (T_g = 76 K) and methylcyclohexane (T_g = 85 K), and the T_g of benzyl alcohol (T_g = 171 K) is higher than the T_g of toluene (T_g = 115 K). For saturated hydrocarbons, the primary factor determining the T_g is clearly molecular size. The SC-1 LR with 32 hydrocarbons (in Tables 1 and 2) could reproduce

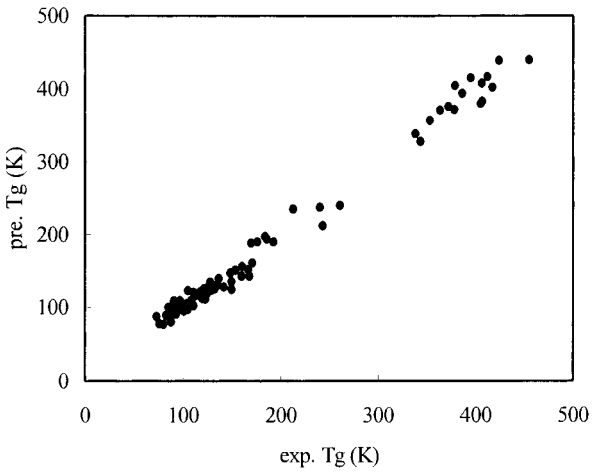

Figure 2. Plot of observed versus predicted T_g for the 81 training compounds set using MLR.

the experimental T_g well, R^2 = 0.923 and AE = 9.4 K. Especially, the R^2 and the AE for 18 aliphatic hydrocarbons are 0.94 and 7.5 K, respectively.

The best correlation for T_g expressed with the MLR equation contains seven descriptors from five descriptor groups. The MLR representation of the T_g is as follows:

$$T_g = 10.86\mathrm{SC\text{-}1} + 18.72\mathrm{RoG} - 9.738\mathrm{AlogP} - 0.605\mathrm{WNSA\text{-}1} - 26.25\mathrm{FPSA\text{-}2} + 0.284\mathrm{TPSA} + 17.05\mathrm{HBC} + 51.1091 \quad (2)$$

This MLR equation can reproduce the T_g of the training set very well, R^2, R_{cv}^2 and AE are 0.989, 0.985, and 8.8 K, respectively. In Table 1, the calculated and the experimental T_g are listed for the 81 training set and are plotted in Figure 2. According to the eq 2, T_g of organic solids influenced mainly by the molecular size, the molecular shape, and the intermolecular interaction.[16]

Since the freezing of the rotational motion of the molecule in a solid was the correlation influenced by the shape, the radius of gyrations works as an impact descriptor in the T_g expression. The T_g correlates with the radius of gyration (RoG) of 0.93.

The correlation coefficient between AlogP value and T_g is 0.89. The AlogP is the logarithm of the partition coefficient of the compound between 1-octanol and water, which increases as the ratio of the nonpolar group in a molecule increases. Since the compounds with polar groups have a negative or smaller AlogP value, the coefficient of AlogP in the eq 2 has a negative sign.

Therefore, the value of AlogP reflects these influences; that is, the methylene group that attached to a basic hydrocarbon, the hydrogen bonding generating group such as −OH, halogen atoms, and aromatic ring effect the T_g value.

The three charged surface descriptors, WNSA-1, TPSA, and FPSA-2, also have high correlation with the T_g. Since these descriptors depend on each other, it is not necessary to describe the influence of each descriptor on the T_g. Both WNSA-1 and FPSA-2 have high R^2 where as TPSA has low R^2. Since the motion of the molecule in the solid phase, especially the rotational motions, is the origin of the T_g, the physical properties that influence the molecular rotation in the solid phase can be good descriptors for describing the

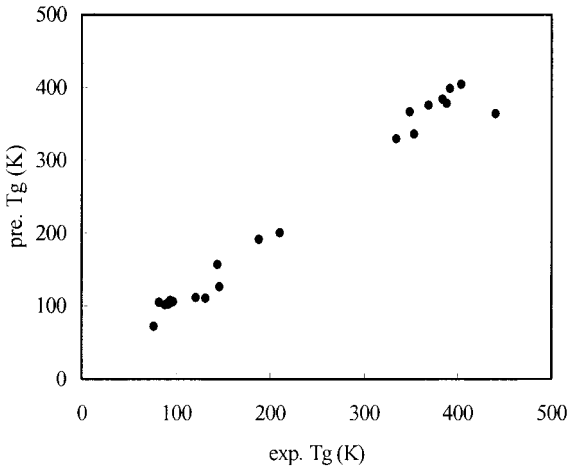

Figure 3. Plot of observed versus predicted T_g for the 22 compounds in prediction set.

T_gs of organic solids. In molecular solids, the intermolecular attractions prevent the molecule from rotating at its equilibrium position. The shape of the molecule, SC-1 and RoG in eq 2, are also important factors for the rotational motion in the solid. The descriptors which contain the information about the polarity of the molecule, AlogP, WNSA-1, FPSA-2, and TPSA, are responsible for the representation of polar intermolecular interactions. So, they are necessary for separate treatment of these hydrogen atoms.

Since the hydrogen bond effect cannot be described by the polarity descriptors, the HBC descriptor was selected during the GA procedure to describe the angle dependent short-range attraction. The R^2 value and AE value could be improved by using HBC descriptors. The correlation between HBC and the T_g is very low because all the compounds in the training set do not have H-acceptors or H-donors.

Twenty-seven hydrocarbons and 54 heteroatom containing compounds are included in the training set. Sixteen LED materials are included in the heteroatom containing compounds. Comparing average errors of these classes, the AE of the hydrocarbon compounds ($n = 27$) is 6.6 K, the AE of the heteroatom containing compounds ($n = 38$), excluding LED materials, is 9.0 K, and the AE of LED materials ($n = 16$) is 12.0 K.

For the prediction set, the AE of the predicted T_g is 13.9 K, and the R^2 is 0.976 (Table 2). Five hydrocarbons, 17 heteroatom containing compounds, and 8 LED materials are included in the prediction set. The predicted vs experimental T_g are plotted in Figure 3.

The AE of the T_g of the LED materials is obtained as 17.6 K. In particular, the error of compound no. 100 (EM5 in Figure 1) is 76 K, which is much larger than the AE (17.6 K). Except for compound no. 100, the AE of the LED materials is 9.2 K.

From the analysis of the eq 2, it is evident that the T_g of a molecule can be described by the descriptors that are responsible for the motion of the molecule in the condensed phase, the size (SC-1), shape (RadofGyration), and intermolecular interaction (AlogP, HBC, WNSA-1, FPSA-1, TPSA).

CONCLUSION

A QSPR model was used to predict the T_g of organic compounds with properties derived from the structures of molecules. After being analyzed by MLR using seven descriptors, on the 81 training set, R^2 value was obtained as 0.989, and the average error was 8.8 K. For the 22 compounds prediction set, R^2 was 0.976, and the AE was 13.9 K. Since the T_g is closely related to the rotational motion of the molecule in a solid, the descriptors that are related to the rotational motions in the solid were selected through GA procedure.

For the saturated hydrocarbons, the major factor determining the T_g is molecular size and shape.

The descriptors in the MLR model are the number of bonds, radius of gyration, HBC, AlogP, and three descriptors that represent the polarity of the molecule. The number of bonds and the radius of gyration describe the size and shape. The strength of the intermolecular interaction is described with WNSA-1, FPSA-2, TPSA, and the hydrogen bond also plays an important role to prevent molecular rotation.

We proposed a physically realistic MLR model to describe T_g. With this model, one can easily estimate the T_g of organic solids and especially the T_g of LED materials.

ACKNOWLEDGMENT

Y. S. Kim thanks research workers in the Computer Aided Molecular Design Research Center at Soong Sil University for the technical advice. This work was supported in part by Korea Research Foundation Grant (KRF-99-005-D00075), the Korea Research Center for Theoretical Physics and Chemistry, Korea Research Foundation Grant (KRF-1997-012-D00035), and Hyperstructured Organic Materials Research Center (HOMRC).

REFERENCES AND NOTES

(1) Rickey, J. S. American Society for Testing and Materials. *Assignment of the glass transition*; American Society for Testing and Materials: Philadelphia, PA, 1994.
(2) Barton, J. M. Relation of Glass Transition Temperature to Molecular Structure of Addition Copolymers. *J. Polym. Sci., Part C* **1970**, *30*, 573−597.
(3) Van Kervelen D. W. *Properties of Polymers: Their Correlation with Chemical Structure; Their Numerical Estimation and Prediction from Additive Group Contributions*; Elsevier: Amsterdam, 1990.
(4) Hopfinger, A. J.; Koehler, M. G.; Pearlstein, R. A. Molecular Modeling of Polymers. Estimation of Glass Transition Temperatures. *J. Polym. Sci., Polym. Phys. Ed.* **1988**, *26*, 2007−2028.
(5) Hopfinger, A. J.; Koehler, M. G. In *Computer Simulation of Polymers*; Collbourn, E., Ed.; Polymer Science and Technology Series, Longman Scientific & Technical: London, 1994; pp 1−44.
(6) Lee, W. A. Calculation of the Glass Transition Temperatures of Polymers. Part I. Homopolymers and Copolymers with Alkyl Side Chains. *J. Polym. Sci., Part A-2* **1970**, *8*, 555−570.
(7) Biceano, J. *Computational Modeling of Polymers*; M. Dekker. Inc.: New York, 1992.
(8) Camelio, P.; Lazzeri, V.; Waegell, B. *Polym. Prep*. (Am. Chem. Soc., Div. Polym. Chem.) **1995**, *36*, 661.
(9) Camelio, P. Master's thesis, Faculté des Sciences et Techniques de Saint-Jérôme, Marseille (Juin 1994), D.E.A. "Synthèse et Modélisation de Molécules Bioactives."
(10) Camelio, P.; Cypcar, C. C.; Lazzeri, V.; Waegell, B. A Novel Approach Toward the Prediction of the Glass Transition Temperature; Application of the EVM Model, a Designer QSPR Equation for the Prediction of Acrylate and Methacrylate Polymers. *J. Polym. Sci.* **1997**, *35*, 2579−2590.
(11) Cypcar, C. C.; Camello, P.; Lazzeri, V.; Mathias, L. J.; Waegell, B. Prediction of the Glass Transition Temperature of Multicyclic and Bulky Substituted Acrylate and Methacrylate Polymers Using the Energy, Volume, Mass(EVM) QSPR Model. *Macromolecules* **1996**, *29*, 8954−8959.
(12) Stacey Fu, C. Y.; Lackritz, H. S.; Priddy, D. B., Jr.; McGrath, J. E. Polymer Physics and Structure/Property Relationships of Thermally Stable Polyarylene Ethers for Second-Order Nonlinear Optics. *Chem. Mater*. **1996**, *8*, 514−525.

(13) Katrizky, A. R.; Rachwal, P.; Law, K. W.; Karelson, M.; Lobanov, V. S. Prediction of Polymer Glass Transition Temperatures Using a General Quantitative Structure−Property Relationship Treatment. *J. Chem. Inf. Comput. Sci.* **1996**, *36*, 879−884.
(14) Carrard, M.; Goncalves-Conto, S.; Si-Ahmed, L.; Adès, D.; Siove, A. Improved stability of interfaces in organic light emitting diodes with high T_g materials and self-assembled monolayers. *Thin Solid Films* **1999**, *352*, 189−194.
(15) Tokito, S.; Tanaka, H.; Okada, A.; Taga, Y. High-temperature operation of an electroluminescent device fabricated using a novel triphenylamine derivative. *Appl. Phys. Lett.* **1996**, *69*, 878−880.
(16) Halgren, T. A. Merck Molecular Force Field. I. Basis, Form, Scope. Parametrization, and Performance of MMFF94. *J. Comput. Chem*. **1996**, *17*, 490
(17) Angell, C. A.; Sare, J. M.; Sare, E. J. Glass Transition Temperatures for Simple Molecular Liquids and Their Binary Solutions. *J. Phys. Chem*. **1978**, *24*, 2622−2629.
(18) Yamamuro, O.; Ishikawa, M.; Kisimoto, I. Thermodynamic Approach to Glass Transitions of Plastically Crystalline Cyanoadamantane and Isocyanocyclohexane. *J. Phys. Soc. Jpn.* **1999**, *68*, 2969−2976.
(19) Carpenter, M. R.; Davies, D. B.; Matheson, A. J. Measurement of the Glass-Transition Temperature of Simple Liquids. *J. Chem. Phys*. **1967**, *46*, 2451−2454.
(20) Angell, C. A. Relaxation in liquids, polymers and plastic crystals − strong/fragile patterns and problems. *J. Non-Crystalline Solids* **1991**, *131*, 13−31.
(21) Dries, T.; Fujara, F.; Kedbel, M.; Rossler, E.; Sillescu, H. ^{2}H NMR study of the glass transition in supercooled ortho-terphenyl. *J. Chem. Phys.* **1988**, *88*, 2139−2147.
(22) Lesikar, A. V. On the glass transition in mixtures between the normal alcohols and various Lewis bases. *J. Chem. Phys*. **1977**, *66*, 4263−4276.
(23) Sutter, E. J.; Angell, C. A. Glass Transitions in Molecular Liquids. I. Influence of Proton-Transfer Processes in Hydrazine-Based Solutions. *J. Phys. Chem*. **1971**, *75*, 1826−1832.
(24) Pissis, P.; Apekis, L. A dielectric study of molecular mobility at glass transition. *J. Non-Crystalline Solids* **1991**, *131*, 95−98.
(25) Cukierman, M.; Lane, J. W.; Uhlmann, D. R. High − temperature flow behavior of glass-forming liquids: A free-volume interpretation. *J. Chem. Phys*. **1973**, *59*, 3639−3644.
(26) Kishimoto, K.; Suga, H.; Seki, S. Calorimetric Study of the Glassy State. XIV. Calorimetric Study on Unusual Glass Transition Phenomena in $CFCl_2$−$CFCl_2$. *Bull. Chem. Soc. Jpn.* **1978**, *51*, 1691−1696.
(27) Lesikar, A. V. On the glass transition in organic halide-alcohol mixtures. *J. Chem. Phys.* **1975**, *63*, 2297.
(28) Börjesson, L.; Howells, W. S. Incoherent quasi-elastic neutron scattering of propylene carbonate in the glass instability range. *J. Non-Crystalline Solids* **1991**, *131*−*133*, 53−57.
(29) Meier, G.; Gerharz, B.; Boese, D. Dynamical processes in organic glass-forming van der Waals liquids. *J. Non-Crystalline Solids* **1991**, *131*, 144−152.
(30) Hu, N. X.; Xie, S.; Popovic, Z.; Ong, B.; Hor, A. M. Novel High T_g Hole Transport Molecules for Organic Electroluminescent Devices. *Proceedings of the Fifth International Display Workshops;* 1998; pp 863−864.
(31) Ogawa, H.; Ohnishi, K.; Shirota, Y. Tri(p-terphinyl-4-yl)amine as a novel blue-emitting material for organic electroluminescent devices. *Synthetic Metals* **1997**, *91*, 243−245.
(32) Antoniadis, H.; Inbasekaran, M.; Woo, E. P. Blue-green organic light-emitting diodes based on fluorene-oxadiazole compounds. *Appl. Phys. Lett*. **1998**, *73*, 3055−3057.
(33) Tamot, N.; Adachi, C.; Nagai, K. Electroluminescence of 1,3,4-Oxadiazole and Triphenylamine-Containing Molecules as an Emitter in Organic Multilayer Light Emitting Diodes. *Chem. Mater*. **1997**, *9*, 1077−1085.
(34) Shirota, Y.; Kuwabara, Y.; Okuda, D.; Okuda, R.; Ogawa, H.; Inada, H.; Kakada, H.; Yonemoto, Y.; Kawami, S.; Imai, K. Starburst molecules based on p-electron systems as materials of organic electroluminescent devices. *J. Luminescence* **1997**, *72*−*74*, 985−991.
(35) Murata, H.; Merritt, C. D.; Inada, H.; Shirota, Y.; Kafafi, Z. H. Molecular organic light-emitting diodes with temperature-Independent quantum efficiency and improved thermal durability. *Appl. Phys. Lett*. **1999**, *75*, 3252−3254.
(36) Fink, R.; Heischkel, Y.; Thelakkat, M.; Schmidt, H. W.; Jonda, C.; Hüppauff, M. Synthesis and Application of Demiric 1,3,5-Triazine Ethers as Hole-Blocking Materials in Electroluminescent Devices. *Chem. Mater*. **1995**, *10*, 3620−3625.
(37) Wiener, J. Structural Determination of Paraffin Boiling Points. *J. Am. Chem. Soc.* **1947**, *69*, 17−20.
(38) Randic, M. On Characterization of Molecular Branching. *J. Am. Chem. Soc.* **1975**, *97*, 6609−6615.
(39) Kier, L. B.; Hall, L. H. *Molecular Connectivity on Chemistry and Drug Research*; Academic Press: New York, 1976.
(40) Stanton, D. T.; Jurs, P. C. Development and Use of Charged Partial Surface Area Structural Descriptors in Computer-Assisted Quantitative Structure−Property Relationship Studies. *Anyl. Chem.* **1990**, *62*, 2323−2329.
(41) Johnson, S. R.; Jurs, P. C. Prediction of the clearing temperatures of a series of liquid crystals from molecular structure. *Chem. Mater.* **1999**, *11*, 1007−1023.
(42) Luke, B. T. Evolutionary programming applied to the development of quantitative structure−activity relationships and quantitative structure−property relationships. *J. Chem. Inf. Comput. Sci.* **1994**, *34*, 1279−1287.

CI0103018